1521-0103/378/1/10–19$35.00
THE JOURNAL OF PHARMACOLOGY AND EXPERIMENTAL THERAPEUTICS

https://doi.org/10.1124/jpet.121.000539
J Pharmacol Exp Ther 378:10–19, July 2021

Rosuvastatin Inhibits the Apoptosis of Platelet-Derived Growth Factor–Stimulated Vascular Smooth Muscle Cells by Inhibiting p38 via Autophagy

Jun-Hwan Jo, Hyun-Soo Park, Do-Hyung Lee, Joo-Hui Han, Kyung-Sun Heo, and Chang-Seon Myung

Department of Pharmacology, Chungnam National University College of Pharmacy, Daejeon, Republic of Korea

Received for publication January 27, 2021; accepted for publication April 06, 2021

ABSTRACT

The secretion of platelet-derived growth factors (PDGFs) into vascular smooth muscle cells (VSMCs) induced by specific stimuli, such as oxidized low-density lipoprotein (LDL) cholesterol, initially increases the proliferation and migration of VSMCs, and continuous stimulation leads to VSMC apoptosis, resulting in the formation of atheroma. Autophagy suppresses VSMC apoptosis, and statins can activate autophagy. Thus, this study aimed to investigate the mechanism of the autophagy-mediated vasoprotective activity of rosuvastatin, one of the most potent statins, in VSMCs continuously stimulated with PDGF-BB, a PDGF isoform, at a high concentration (100 ng/ml) to induce phenotypic switching of VSMC. Rosuvastatin inhibited apoptosis in a concentration-dependent manner by reducing cleaved caspase-3 and interleukin-1β (IL-1β) levels and reduced intracellular reactive oxygen species (ROS) levels in PDGF-stimulated VSMCs. It also inhibited PDGF-induced p38 phosphorylation and increased the expression of microtubule-associated protein light chain 3 (LC3) and the conversion of LC3-I to LC3-II in PDGF-stimulated VSMCs. The ability of rosuvastatin to inhibit apoptosis and p38 phosphorylation was suppressed by treatment with 3-methyladenine (an autophagy inhibitor) but promoted by rapamycin (an autophagy activator) treatment. SB203580, a p38 inhibitor, reduced the PDGF-induced increase in intracellular ROS levels and inhibited the formation of cleaved caspase-3, indicating the suppression of apoptosis. In carotid ligation model mice, rosuvastatin decreased the thickness and area of the intima and increased the area of the lumen. In conclusion, our observations suggest that rosuvastatin inhibits p38 phosphorylation through autophagy and subsequently reduces intracellular ROS levels, leading to its vasoprotective activity.

SIGNIFICANCE STATEMENT

This study shows the mechanism responsible for the vasoprotective activity of rosuvastatin in vascular smooth muscle cells under prolonged platelet-derived growth factor stimulation. Rosuvastatin inhibits p38 activation through autophagy, thereby suppressing intracellular reactive oxygen species levels, leading to the inhibition of apoptosis and reductions in the intima thickness and area. Overall, these results suggest that rosuvastatin can be used as a novel treatment to manage chronic vascular diseases such as atherosclerosis.

Introduction

In addition to stroke and myocardial infarction, atherosclerosis has a high mortality rate throughout the world, and the leading cause of atherosclerotic lesions is low-density lipoprotein (LDL) cholesterol, through which cholesterol is transported through blood vessels (Libby et al., 2019). Complex interactions between vascular smooth muscle cell (VSMC) proliferation and other processes are characteristic of atherosclerotic lesions; lipid deposition in parts of the arteries and endothelial dysfunction lead to the formation of atherosclerotic intima plaques (Lim and Park, 2014). In the progression of atherosclerosis, oxidized LDL cholesterol accumulates in the intima and induces the entrance of monocytes, which are transformed into macrophages that absorb oxidized LDL cholesterol, developing into foam cells that subsequently secrete platelet-derived growth factor (PDGF) and inflammatory cytokines (Oishi and Manabe, 2016; Cervantes Gracia et al., 2017).

The PDGF-mediated signaling pathway is activated by the binding of each PDGF protein isoform (PDGF-AA, -AB, -BB, -CC, and -DD) to the PDGF receptor. PDGF-BB is one of the most important stimulators of VSMC proliferation and migration in damaged blood vessels (Liu et al., 2005; Ha et al., 2015). Plasma PDGF (PDGF-BB + PDGF-AB) levels were 0.45 ± 0.14 ng/ml in healthy subjects (22), and in patients with essential hypertension (25), these levels increased to 0.63 ±

This work was supported by the National Research Foundation of Korea (KRF), funded by the Ministry of Science and ICT [Grant NRF-2018R1A2A2A05023578].

No author has an actual or perceived conflict of interest with the contents of this article.

dx.doi.org/10.1124/jpet.121.000539.

ABBREVIATIONS: DMEM, Dulbecco's modified Eagle's medium; DPPH, 2,2-diphenyl-1-picrylhydrazyl; ERK1/2, extracellular signal–regulated kinase 1/2; FITC, fluorescein isothiocyanate; H_2DCFDA, 2′,7′-dichlorofluorescin diacetate; IL-1β, interleukin 1β; LC3, microtubule-associated proteins 1A/1B light chain 3B; LCA, left carotid artery; LDL, low-density lipoprotein; 3-MA, 3-methyladenine; MTT, 3-(4,5-dimethylthiazol-2-yl)-2,5-diphenyltetrazolium bromide; NAC, *N*-acetyl-L-cysteine; PDGF, platelet-derived growth factor; ROS, reactive oxygen species; VSMC, vascular smooth muscle cell; WST, water-soluble tetrazolium.

0.23 ng/ml (Rossi et al., 1998). In addition, excessive and prolonged PDGF-BB stimulation induces apoptosis by producing reactive oxygen species (ROS) (Okura et al., 1998; Park et al., 2018), and apoptosis causes secondary necrosis as a result of the absence of effective phagocytosis, leading to an increase in plaque rupture by cap thinning (Bennett et al., 2012; Bennett et al., 2016). Therefore, suppression of apoptosis induced by excessive and prolonged stimulation of PDGF-BB is essential for preventing and treating atherosclerosis.

Autophagy is a phenomenon in which cell components such as lipids, proteins, and damaged organelles are recycled through the lysosomal degradation pathway (Yang et al., 2015). Target molecules are sequestered and accumulate in a double-membrane organelle called the autophagosome; the autophagosome then fuses with the lysosome, after which the target molecules are decomposed and their components are recycled (Levine and Kroemer, 2019). In autophagy, microtubule-associated proteins 1A/1B light chain 3B (LC3) are mainly used as a biomarker (Pugsley, 2017). LC3 is one of the essential substances that form autophagosomes, and LC3 is synthesized and then processed into LC3-I and converted into LC3-II (Tanida et al., 2008). The conversion of LC3-I to LC3-II is related to the extent of autophagosome formation (Kabeya et al., 2000), which means autophagy. Therefore, the measurement of conversion of LC3-I to LC3-II is commonly used for experimental autophagy activity (Park et al., 2018). Autophagy was reported to inhibit apoptosis in blood vessels and protect blood vessels by reducing ROS in PDGF-BB–stimulated VSMCs (Park et al., 2018); therefore, autophagy may be an important therapeutic target for the protection of blood vessels.

Statins, which are used to inhibit cholesterol synthesis by inhibiting 3-hydroxy-3-methyl-glutaryl-CoA reductase, are known to have a wide range of effects, such as their anti-inflammatory, angiogenic, and vasoprotective effects (Soulaidopoulos et al., 2018). Statins have also been reported to regulate autophagy (Altwairgi, 2015); however, the exact mechanism of their vasoprotective activity through autophagy is undefined. Thus, this study aimed to clarify the regulatory effect of rosuvastatin, the most potent statin in reducing LDL cholesterol (Lopez, 2005; Karlson et al., 2016), on apoptosis via autophagy in PDGF-stimulated VSMCs. For this purpose, we stimulated VSMCs cultured at maximal confluency with excessive PDGF-BB to induce cell death.

Materials and Methods

Reagents and Antibodies. Dulbecco's modified Eagle's medium (DMEM), FBS, trypsin-EDTA, PBS, and penicillin/streptomycin were obtained from Gibco Inc. (Grand Island, NY). 2′,7′-Dichlorofluorescin diacetate (H_2DCFDA), 2,2-diphenyl-1-picrylhydrazyl (DPPH), 3-(4,5-dimethylthiazol-2-yl)-2,5-diphenyltetrazolium bromide (MTT), *N*-acetyl-L-cysteine (NAC), and SB203580 were purchased from Sigma-Aldrich (St. Louis, MO). 3-Methyladenine (3-MA) and rapamycin were obtained from Merck Millipore (Billerica, MA). Anti–interleukin-1β (IL-1β) and mouse anti-rabbit IgG-FITC were obtained from Santa Cruz Biotechnology (Dallas, TX). Anti–β-actin and goat anti-rabbit were purchased from AbFrontier (Geumcheon, Seoul, Korea). Anti–phospho-extracellular signal–regulated kinase 1/2 (ERK1/2), anti-ERK1/2, anti–phospho-p38, anti-p38, anti–caspase-3, and anti-LC3 antibodies were obtained from Cell Signaling Technology (Beverly, MA). Rosuvastatin was obtained from Cayman Chemical (Ann Arbor, MI). PDGF-BB was purchased from Pepro Tech (Rocky Hill, NJ).

Cell Culture. Rat aortic VSMCs (Cell Applications, Inc.) were cultured in DMEM with 10% FBS, 4.5 g/l D-glucose, 1% penicillin/streptomycin, 2 mM L-glutamine, and 100 mg/l sodium pyruvate at 37°C in a humidified incubator under 5% CO_2. Prior to all experiments, the VSMCs were cultured to full confluency on plates. The experiment was conducted with VSMCs at passages 5–10.

Animals. Male C57BL/6 mice at 6 weeks of age (23–25 g) were purchased from Samtako (Osan, Korea) and used to evaluate the vasoprotective activities of rosuvastatin. Prior to the experiment, the animals were acclimated for 1 week. All experimental procedures using animals were performed according to the guidelines of the Chungnam National University Ethics Committee (CNU-00967; Daejeon, Korea).

Carotid Ligation and Drug Dosing. A carotid ligation model was induced using male C57BL/6 mice. The mice were anesthetized by intraperitoneal injection of 50 mg/kg pentobarbital, and anesthetization was maintained through inhalation of 2.5% isoflurane with oxygen. Afterward, the left carotid artery (LCA) was exposed and completely ligated. Ligation proceeded when there was no physical movement after anesthesia. The mice were treated with 1% ketoprofen to ensure their pain-free recovery. After 5 weeks, the mice were sacrificed through excess pentobarbital, and the carotid arteries and other organs (lung, heart, liver, kidney, and spleen) were harvested and fixed in paraffin. The animals were randomly divided into four groups. Animals in the drug-treated experimental groups were orally administered 1 or 10 mg/kg rosuvastatin per day (n = 7 per group), and normal saline was administered to both normal mice and model mice subjected to carotid ligation (n = 8 per group). Rosuvastatin was administered once a day beginning 2 days before LCA ligation until 5 weeks after ligation.

Histologic Analysis. Serial cross sections (5-μm thickness) throughout the entire length of the LCA were obtained, and staining was performed using H&E (Heo et al., 2014). Computerized morphometric analysis (Image J software; National Institutes of Health, MD) was used to determine the thickness and area of the intima and media.

Cell Viability Assay. An MTT assay was performed to find the concentration ranges of rosuvastatin and SB203580, which can be used in VSMCs without cytotoxicity. VSMCs were seeded in 96-well plates at a density of 1×10^4 cells per well and cultured in DMEM containing 10% FBS at 37°C and 5% CO_2. After 48 hours, the VSMCs were treated with 2.5–100 μM rosuvastatin, 5 or 10 μM SB203580, and 100 μg/ml digitonin (a positive control) in 0.1% FBS-containing DMEM for 120 or 96 hours. After the culture period, 200 μl of a 5-mg/ml MTT solution was added to each well and incubated for 4 hours. After the MTT solution was removed, 200 μl of DMSO was added to each well. The absorbance at 565 nm was measured with an Infinite M Nano microplate reader (Tecan Group Ltd., Männedorf, Switzerland).

A water-soluble tetrazolium (WST)-8 assay was performed to evaluate the effects of rosuvastatin on cell viability in VSMCs stimulated with PDGF-BB. Because the WST-8 assay does not use DMSO, possible cell damage by DMSO can be excluded, and cell viability can be measured more precisely due to its high sensitivity. VSMCs were seeded in 96-well plates at a density of 4×10^4 cells/ml and incubated with DMEM containing 10% FBS at 37°C and 5% CO_2 for 48 hours. The cells were pretreated with 10 or 40 μM rosuvastatin for 24 hours, and 10 or 100 ng/ml PDGF-BB was added for 24–96 hours. Treatment with rosuvastatin and PDGF-BB was followed by culture in DMEM containing 0.1% FBS. After the reaction, 100 μl of Quanti-Max WST-8 solution (Biomax, Nowon, Seoul, Korea) was added to the plate. VSMCs were incubated at 37°C and 5% CO_2 for 1 hour. The absorbance at 450 nm was then determined using an Infinite M Nano microplate reader (Tecan Group Ltd.).

Cell Apoptosis Assay. The cell apoptosis level was evaluated using the Muse Annexin V & Dead Cell Kit from Merck Millipore (Billerica, MA). VSMCs were seeded in 12-well plates at a density of 1.8×10^5 cells per well and incubated in DMEM containing 10% FBS for 42 hours. Subsequently, cells were pretreated with 10 or 40 μM rosuvastatin, 100 nM rapamycin, and 50 mM 3-MA for 24 hours; 10 or

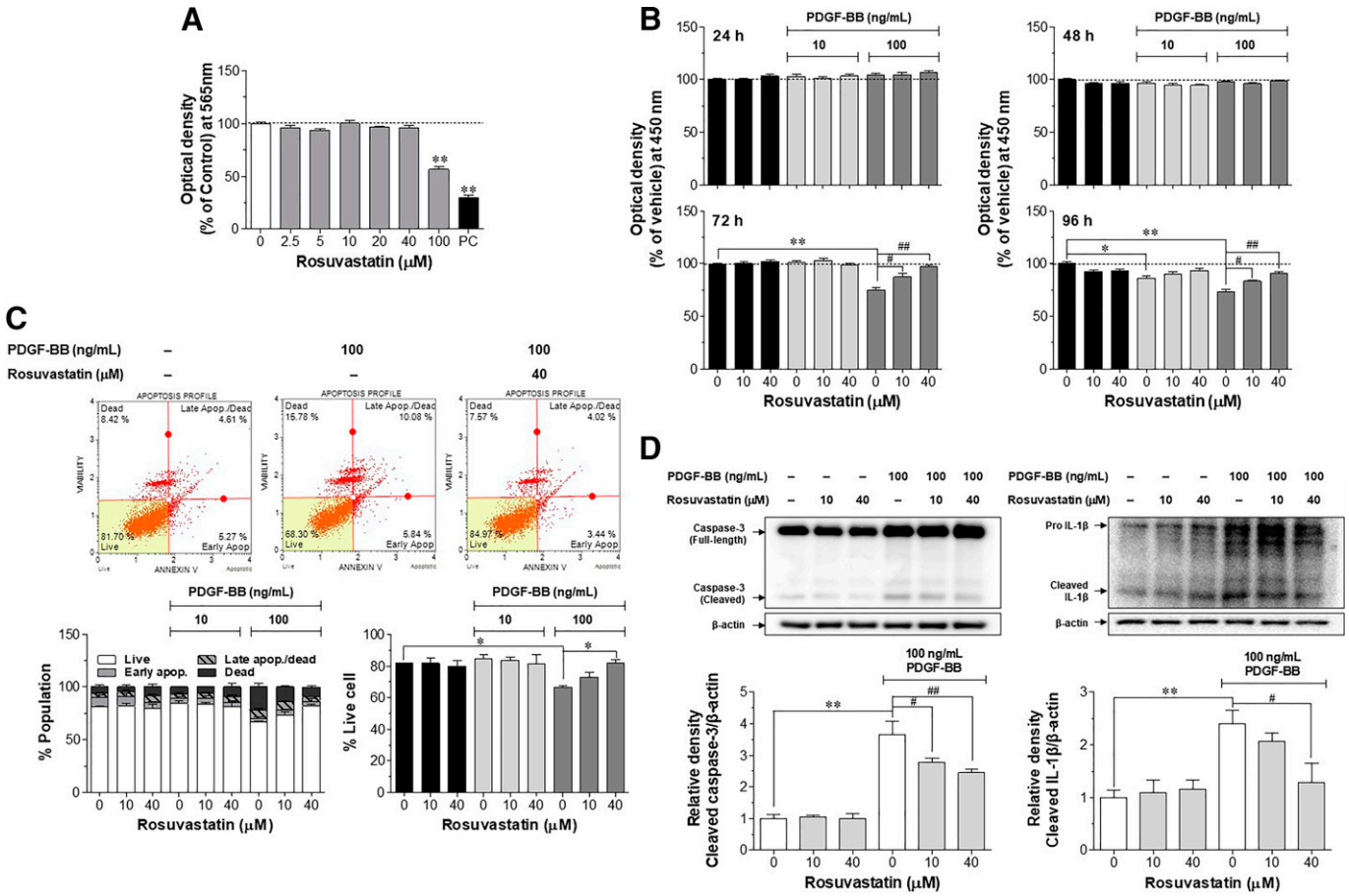

Fig. 1. Effect of rosuvastatin on the viability of VSMCs stimulated by PDGF. (A) The concentration of rosuvastatin used for subsequent experiments was determined through MTT assay. VSMCs were treated with rosuvastatin (2.5–100 μM) for 120 hours. Digitonin (100 μg/ml) was used as a positive control (PC). (B) VSMCs were treated with rosuvastatin (10 or 40 μM) for 24 hours, after which PDGF-BB (10 or 100 ng/ml) was added for an additional 24, 48, 72, or 96 hours. VSMC viability was measured via WST-8 assay. (C) VSMC death was evaluated using the Muse Annexin V & Dead Cell assay. (D) The expression of cleaved caspase-3 (a key marker of cell apoptosis) and IL-1β (a key marker of secondary necrosis by apoptosis) was measured via Western blot analysis. The gel images are representative of three similar independent experiments. Data are expressed as the mean ± S.E.M. $^{*}P < 0.05$; $^{**}P < 0.01$ vs. no treated control, $^{\#}P < 0.05$; $^{\#\#}P < 0.01$ vs. PDGF-BB (100 ng/ml)–treated control. $n = 3$ per group. apop., apoptosis.

100 ng/ml PDGF-BB was also added for treatment. After 72 hours, the VSMCs were washed in PBS and incubated with 500 μl of a trypsin solution for 3 minutes. The VSMCs were centrifuged at 5000 rpm for 5 minutes. After the supernatant was removed, the pellet was washed with PBS. Staining with Muse Annexin V & Dead Cell Kit solution was then performed in the dark for 10 minutes. Cell apoptosis was measured using a Muse Cell Analyzer from Merck Millipore.

DPPH Assay. A DPPH assay was performed to evaluate the antioxidant activity of rosuvastatin using DPPH solution prepared by mixing methanol and DPPH reagent. DMSO was used as a control, and 10 or 40 μM rosuvastatin and 5 mM NAC (as a positive control) were added to cells seeded in 96-well plates. Subsequently, 100 μl of DPPH solution was added to the cells for incubation in the dark. Using an Infinite M Nano microplate reader (Tecan Group Ltd.), the absorbance at 517 nm was measured. Radical inhibition (%) was calculated using the following equation:

$$\text{Radical inhibition}\,(\%) = \frac{\text{absortance of negative control} - \text{absorbance of sample}}{\text{absorbance of negative control}} \times 100$$

H_2DCFDA Assay. H_2DCFDA was used to determine ROS production in VSMCs; VSMCs were seeded in black 96-well plates at a density of 1×10^4 cells per well and cultured. After 48 hours, the cells were pretreated with 10 or 40 μM rosuvastatin and 5 or 10 μM SB203580 for 24 hours; 10 or 100 ng/ml PDGF-BB was then added for 72 hours of incubation. The VSMCs were washed in PBS and

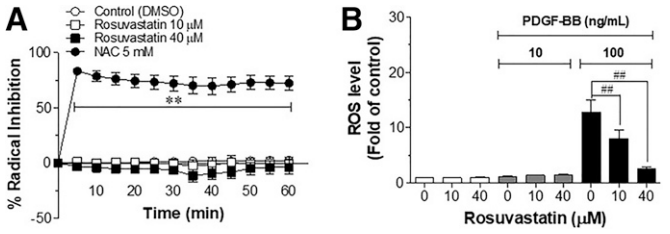

Fig. 2. The free radical scavenging ability of rosuvastatin and its effect on intracellular ROS levels in VSMCs stimulated with PDGF. (A) The DPPH assay was used to assess the free radical scavenging ability of rosuvastatin. The DPPH assay was performed by treating VSMCs with rosuvastatin (10 or 40 μM), DMSO as a control, or NAC (5 mM) as a positive control with 100 μl of a DPPH solution. (B) Rosuvastatin reduced PDGF-BB–stimulated intracellular ROS levels. VSMCs were incubated with rosuvastatin (10 or 40 μM) for 24 hours and additionally treated with PDGF-BB (10 or 100 ng/ml) for 72 hours. VSMCs were treated with H_2DCFDA (20 μM). Data are expressed as the mean ± S.E.M. $^{**}P < 0.01$ vs. DMSO control, $^{\#\#}P < 0.01$ vs. PDGF-BB (100 ng/ml)–treated control. $n = 3$ per group.

incubated with 20 μM H_2DCFDA for 20 minutes at 37°C. The ROS level was measured using an Infinite M Nano microplate reader (Tecan Group Ltd.) at an excitation wavelength of 485 nm and emission wavelength of 540 nm.

Western Blot Analysis. A Western blot analysis was performed to measure protein expression levels. Intact VSMCs were washed in cold PBS and lysed with radioimmunoprecipitation assay buffer [50 mM Tris-HCl (pH 8.0), 150 mM NaCl, 2 mM EDTA, 1 mM sodium

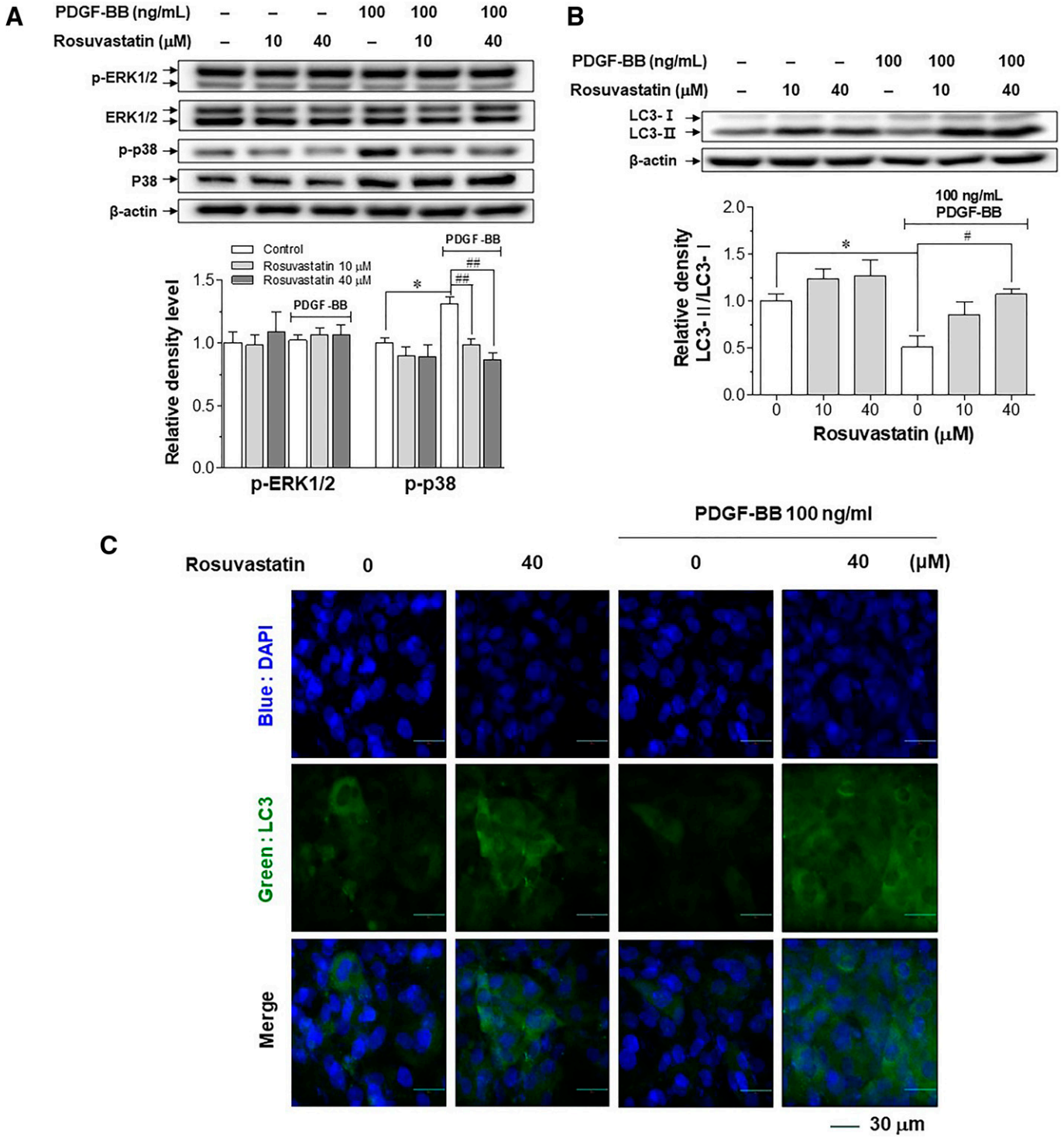

Fig. 3. Effect of rosuvastatin on ERK1/2, p38, and LC3 levels in VSMCs stimulated with PDGF. Protein expression levels were measured using Western blot analysis. VSMCs were incubated with rosuvastatin (10 or 40 μM) for 24 hours and then additionally treated with PDGF-BB (10 or 100 ng/ml) for 72 hours. (A and B) The effects of rosuvastatin on cell growth, apoptosis-associated protein (Erk1/2 and p38) levels, and the conversion of LC3-I to LC3-II in VSMCs stimulated with PDGF-BB are shown. The gel images are representative of three similar independent experiments. Data are expressed as the mean ± S.E.M. $^{*}P < 0.05$ vs. no treated control, $^{\#}P < 0.05$; $^{\#\#}P < 0.01$ vs. PDGF-BB (100 ng/ml)-treated control. (C) LC3 was observed via confocal microscopy. Immunofluorescence staining was conducted with anti-LC3 and anti-FITC secondary antibodies. Cell nuclear staining was performed using 4′,6-diamidino-2-phenylindole (DAPI). Scale bar, 30 μm. $n = 3$ per group. p-ERK1/2, phospho-ERK1/2; p-p38, phospho-p38.

orthovanadate, 1% NP-40, 5 mM NaF, 1 mM phenylmethylsulfonyl fluoride, 0.1% sodium dodecyl sulfate, and 0.5% sodium deoxycholate]. The cell lysate was placed on ice for 30 minutes and centrifuged for 10 minutes at 4°C. The amount of protein was measured with a BCA protein assay kit (Pierce, Rockford, IL). Each protein sample was subjected to SDS-PAGE, and proteins were transferred to a polyvinylidene fluoride membrane (ATTO, Tokyo, Japan). The membrane was washed in T ris-buffered saline/Tween 20 [10 mM Tris (pH 7.6), 0.1% Tween-20, and 150 mM NaCl] for 10 minutes and blocked in Tris-buffered saline/Tween 20 mixed with 5% bovine serum albumin at 4°C for 1 hour. The membrane was then incubated overnight at 4°C with the primary antibody; after washing, the secondary antibody was added and incubated for 6 hours. Chemiluminescence (ECL; ATTO Corp., Tokyo, Japan) was used to detect specific protein signals. Band densities were quantified with ImageJ software (National Institutes of Health, MD).

Immunofluorescence Staining Analysis. Immunofluorescence staining was conducted to measure the expression of LC3 in VSMCs seeded in 24-well plates with coverslips and cultured. After 48 hours, the VSMCs were pretreated with rosuvastatin for 24 hours and additionally treated with PDGF-BB for 72 hours. After the reaction, the cells were washed twice with cold PBS for 10 minutes each and fixed with 4% cold formaldehyde. The cells were permeabilized with PBS containing 0.25% Triton X-100 for 3 minutes and blocked with PBS containing 3% bovine serum albumin at room temperature. The cells were washed after 1 hour with PBS and incubated overnight at 4°C with the primary antibody, followed by additional incubation with anti-FITC antibody at room temperature for 3 hours. The nuclei of the VSMCs were stained using 4′,6-diamidino-2-phenylindole. Images were captured using a confocal laser scanning microscope (K-1 Fluo, Daejeon, Korea).

Statistical Analysis. All data are indicated as the mean ± S.E.M. of three independent experiments. In this study, we used an ANOVA to verify the statistical significance of the differences between means in two or more groups and Dunnett's test to compare each experimental group with a control. All statistical analyses were conducted using GraphPad Prism (San Diego, CA). A P value < 0.05 was considered to indicate a statistically significant difference.

Results

Rosuvastatin Inhibited Apoptosis and the Secondary Necrosis of VSMCs Stimulated with PDGF. VSMCs were pretreated with rosuvastatin before treatment with PDGF-BB, and their increased viability upon rosuvastatin pretreatment was confirmed. The concentration of rosuvastatin used was determined through MTT assay. Rosuvastatin showed no cytotoxicity at concentrations up to 40 μM for 120 hours (Fig. 1A). A WST-8 assay was performed to evaluate the impact of rosuvastatin on cell viability. VSMCs were treated with or without 10 or 40 μM rosuvastatin for 24 hours; 10 or 100 ng/ml PDGF-BB was then added for 24–96 hours of treatment. After PDGF-BB treatment, the viability of VSMCs treated with 100 ng/ml PDGF-BB remained unchanged after 24 hours and 48 hours but decreased beginning at 72 hours of treatment (Fig. 1B). Additionally, rosuvastatin concentration-dependently increased the viability of VSMCs stimulated with PDGF (Fig. 1B). Afterward, cell death was assessed via quantitative analysis and measurement of cleaved caspase-3 expression. The quantitative analysis was performed using the

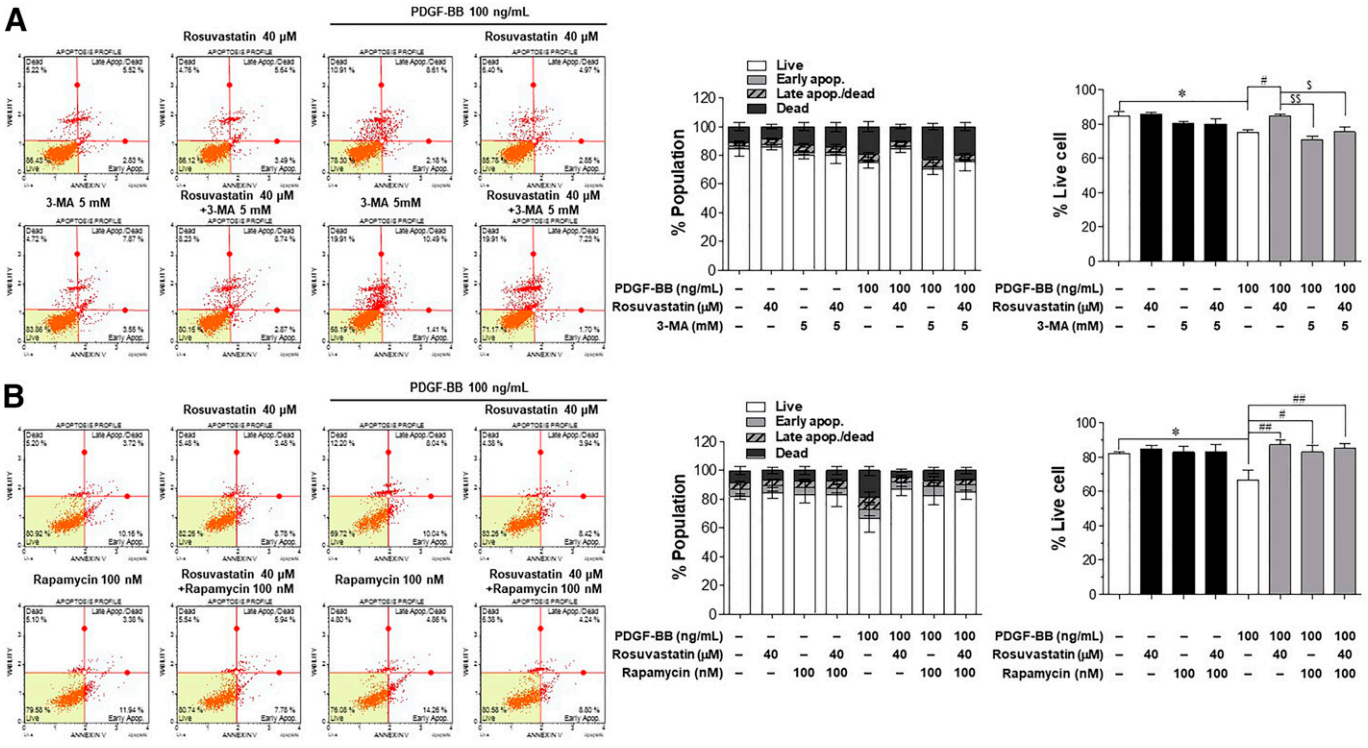

Fig. 4. Antiapoptotic effect of rosuvastatin via autophagy in VSMCs stimulated with PDGF. The antiapoptotic effect of rosuvastatin was confirmed through autophagy inhibition and activation. (A) The autophagy inhibitor 3-MA (5 mM) was used with rosuvastatin (40 μM) to pretreat VSMCs for 24 hours. PDGF-BB (100 ng/ml) was added for an additional 72 hours of treatment. (B) The autophagy activator rapamycin (100 nM) was used with rosuvastatin (40 μM) to pretreat VSMCs for 24 hours. PDGF-BB (100 ng/ml) was added for an additional 72 hours of treatment. The effects of autophagy inhibition (A) and activation (B) on apoptosis were measured through the Muse Annexin V & Dead Cell assay. Data are expressed as the mean ± S.E.M. $^{*}P < 0.05$ vs. no treated control, $^{\#}P < 0.05$; $^{\#\#}P < 0.01$ vs. PDGF-BB (100 ng/ml)–treated control, $^{\$}P<0.05$; $^{\$\$}P <$ 0.01 vs. PDGF-BB (100 ng/ml) + rosuvastatin (40 μM)–treated group. $n = 3$ per group. Apop., apoptosis.

Muse Annexin V & Dead Cell Kit, and the expression of cleaved caspase-3, a critical marker of cell apoptosis (Park et al., 2018), and IL-1β, a critical marker of secondary necrosis (Bennett et al., 2012), was measured using Western blot analysis. In the group incubated with 100 ng/ml PDGF, the increase in cell death induced by PDGF stimulation was inhibited by rosuvastatin in a concentration-dependent manner (Fig. 1C). Rosuvastatin also decreased the expression of cleaved caspase-3 and IL-1β in a concentration-dependent manner (Fig. 1D). These results suggest that rosuvastatin inhibits secondary necrosis by suppressing PDGF-induced apoptosis in VSMCs.

Rosuvastatin Reduced the Intracellular ROS Level in VSMCs Stimulated with PDGF. The DPPH radical assay was used to confirm the antioxidant activity of rosuvastatin. Additionally, the H_2DCFDA assay was performed to measure changes in intracellular ROS levels induced by PDGF stimulation and rosuvastatin treatment in VSMCs. The DPPH assay was performed by treating VSMCs with 10 or 40 μM rosuvastatin, DMSO (control), or 5 mM NAC (positive control) in 100 μl of a DPPH solution. The H_2DCFDA assay was conducted by pretreating VSMCs with 10 or 40 μM rosuvastatin for 24 hours before the addition of 10 or 100 ng/ml PDGF-BB for 72 hours of culture. The results of the DPPH assay showed that rosuvastatin-treated groups exhibited no changes relative to the control group (Fig. 2A). However, in the case of intracellular ROS levels, the group incubated with 100 ng/ml PDGF-BB exhibited increased ROS levels, but ROS levels decreased as the concentration of rosuvastatin increased (Fig. 2B). These results suggest that rosuvastatin has no free radical scavenging activity but reduces the level of intracellular ROS produced by PDGF.

Rosuvastatin Modulated p38 and LC3 in VSMCs Stimulated with PDGF. The expression of apoptosis- and autophagy-associated proteins was quantified to evaluate the effects of rosuvastatin on the mechanisms of apoptosis and autophagy in VSMCs stimulated with PDGF-BB. The phosphorylation of ERK1/2 and p38, which are involved in cell growth and apoptosis (Duan et al., 2016), was measured, and autophagy was confirmed by evaluating the conversion and expression of LC3, a key biologic marker of autophagy (Pugsley, 2017). VSMCs were pretreated with rosuvastatin, after which PDGF-BB was added for additional treatment. The levels of ERK1/2 and p38 were confirmed via Western blot analysis, which showed no change in the level of ERK1/2. However, in the case of p38, its expression was reduced by rosuvastatin (Fig. 3A). Quantitative analysis of LC3 was also conducted using Western blot analysis to measure the conversion of LC3-I to LC3-II. Additionally, LC3 levels in VSMCs were observed via immunofluorescence staining. In the group treated with only 100 ng/ml PDGF-BB, the conversion of LC3-I to LC3-II was decreased; however, in the group pretreated with rosuvastatin, an increase in this conversion was observed (Fig. 3B). Furthermore, compared with the untreated VSMCs, the rosuvastatin-treated VSMCs exhibited increased LC3 expression

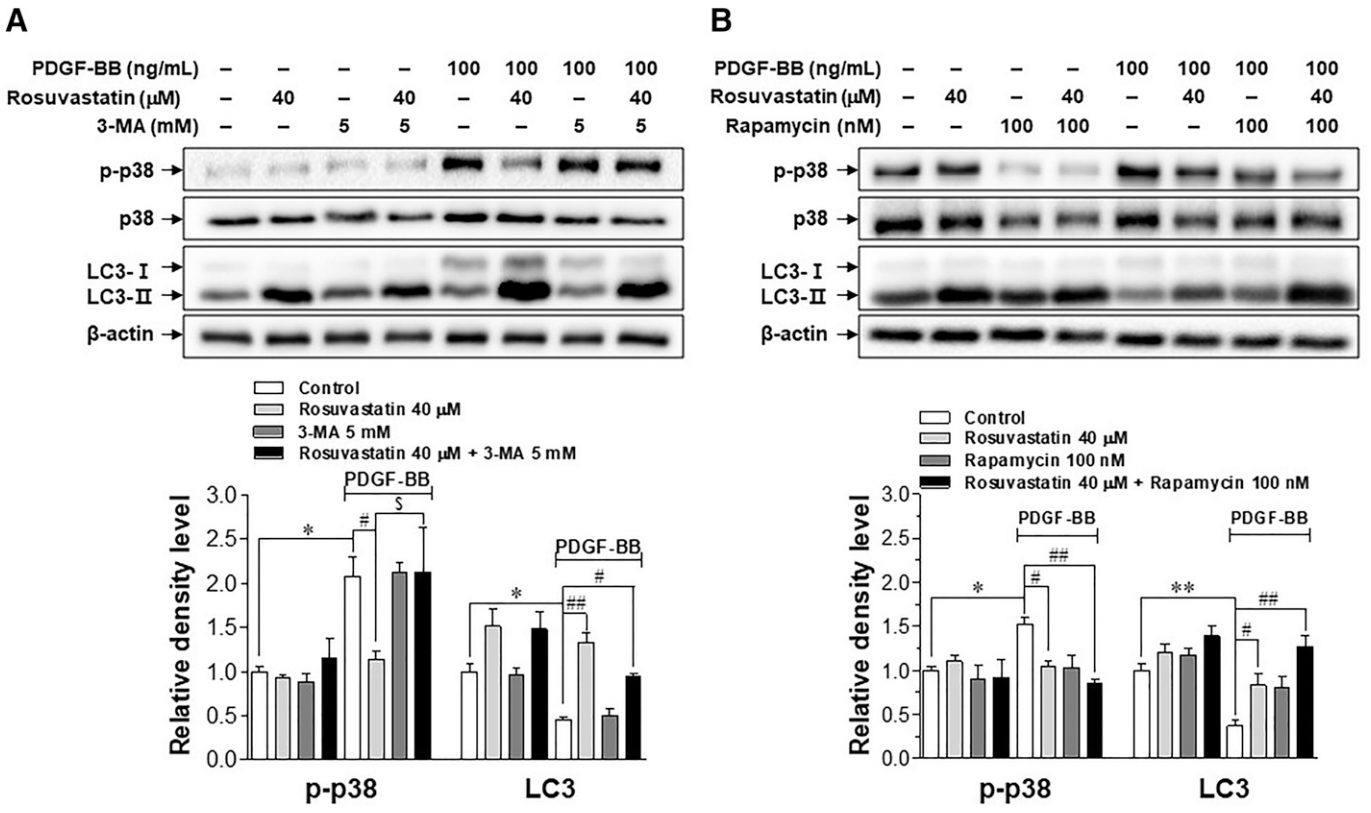

Fig. 5. Effect of rosuvastatin on p38 via autophagy in VSMCs stimulated with PDGF. The effect of rosuvastatin on the activity of p38 was confirmed through autophagy inhibition and activation. (A) The autophagy inhibitor 3-MA (5 mM) was used with rosuvastatin (40 μM) to pretreat VSMCs for 24 hours. PDGF-BB (100 ng/ml) was added for an additional 72 hours of treatment. (B) The autophagy activator rapamycin (100 nM) was used with rosuvastatin (40 μM) to pretreat VSMCs for 24 hours. PDGF-BB (100 ng/ml) was added for an additional 72 hours of treatment. Changes in protein expression due to autophagy inhibition (A) and activation (B) were evaluated via Western blot analysis. The gel images are representative of three similar independent experiments. Data are expressed as the mean ± S.E.M. $^{*}P < 0.05$; $^{**}P < 0.01$ vs. no treated control, $^{\#}P < 0.05$; $^{\#\#}P < 0.01$ vs. PDGF-BB (100 ng/ml)–treated control, $^{\$}P < 0.05$ vs. PDGF-BB (100 ng/ml) + rosuvastatin (40 μM)–treated group. $n = 3$ per group. p-p38, phospho-p38.

(Fig. 3C), indicating that rosuvastatin activates autophagy by increasing the expression and conversion of LC3-I to LC3-II in VSMCs.

Rosuvastatin Reduced Apoptosis through Autophagy in VSMCs Stimulated with PDGF. Quantitative analysis using the Muse Annexin V & Dead Cell Kit was conducted to confirm the role of autophagy in apoptosis in VSMCs stimulated with PDGF-BB. The autophagy activator rapamycin and autophagy inhibitor 3-MA were used at 100 nM and 5 mM, respectively, to treat VSMCs pretreated with 40 μM rosuvastatin for 24 hours. Then, 100 ng/ml PDGF-BB was further added and incubated for 72 hours. For VSMCs in the PDGF group, which were treated with 3-MA and rosuvastatin together, apoptosis increased, and the proportion of live cells decreased compared with that upon treatment with rosuvastatin alone (Fig. 4A). However, when VSMCs were treated with rapamycin, apoptosis decreased, and the proportion of live cells increased (Fig. 4B). These results show that the antiapoptotic effect of rosuvastatin is mediated through autophagic activity.

Rosuvastatin Inhibited the Phosphorylation of p38 through Autophagy in VSMCs Stimulated with PDGF. Western blot analysis of cells treated with rapamycin and 3-MA was performed to confirm the level of autophagy and effect of autophagy on p38. VSMCs were pretreated with 40 μM rosuvastatin, 5 mM 3-MA, and 100 nM rapamycin for 24 hours, after which 100 ng/ml PDGF-BB was added for further treatment of 72 hours. Through measuring the conversion of LC3-I to LC3-II, the effects of 3-MA and rapamycin in promoting and decreasing autophagy were confirmed, and the activity of p38 was also observed. The activity of p38 increased when autophagy was inhibited (Fig. 5A) and decreased when autophagy was activated (Fig. 5B).

Suppression of Intracellular ROS Levels and Apoptosis by p38 Inhibition. SB203580, a specific inhibitor of p38 phosphorylation, was used to treat VSMCs to confirm the regulation of intracellular ROS levels and apoptosis mediated by p38. The MTT assay was used to determine the concentration of SB203580 used in the experiment. The intracellular ROS level, both with and without p38 phosphorylation inhibition, and cleaved caspase-3 expression were confirmed. SB203580 did not show cytotoxicity at concentrations up to 10 μM (Fig. 6A). Therefore, VSMCs were pretreated with 40 μM rosuvastatin and 5 or 10 μM SB203580 for 24 hours. Subsequently, 100 ng/ml PDGF-BB was added for an additional 72 hours. The results showed that SB203580 reduced the intracellular ROS level in PDGF-BB–stimulated VSMCs (Fig. 6B) and decreased the expression of cleaved caspase-3, a key marker of cell apoptosis, in VSMCs stimulated with PDGF (Fig. 6C).

Vasoprotective Effect of Rosuvastatin Shown in a Mouse Model of Carotid Ligation. Carotid ligation has been reported to increase the secretion of inflammatory cytokines and growth factors, thus stimulating the proliferation and migration of VSMCs (Heo et al., 2014). Therefore, a mouse model of carotid ligation was used to evaluate the occurrence of atherosclerosis due to the proliferation and migration of VSMCs. The body weights of the mice were not changed over the experimental period (data not shown), and the thickness and area of the intima and media were measured to determine the effect of rosuvastatin. In the case of media, there was no difference in its thickness or area. However, 10 mg/kg rosuvastatin administration diminished the ligation-induced change in the thickness and area of the intima (Fig. 7). Therefore, a high dose of rosuvastatin

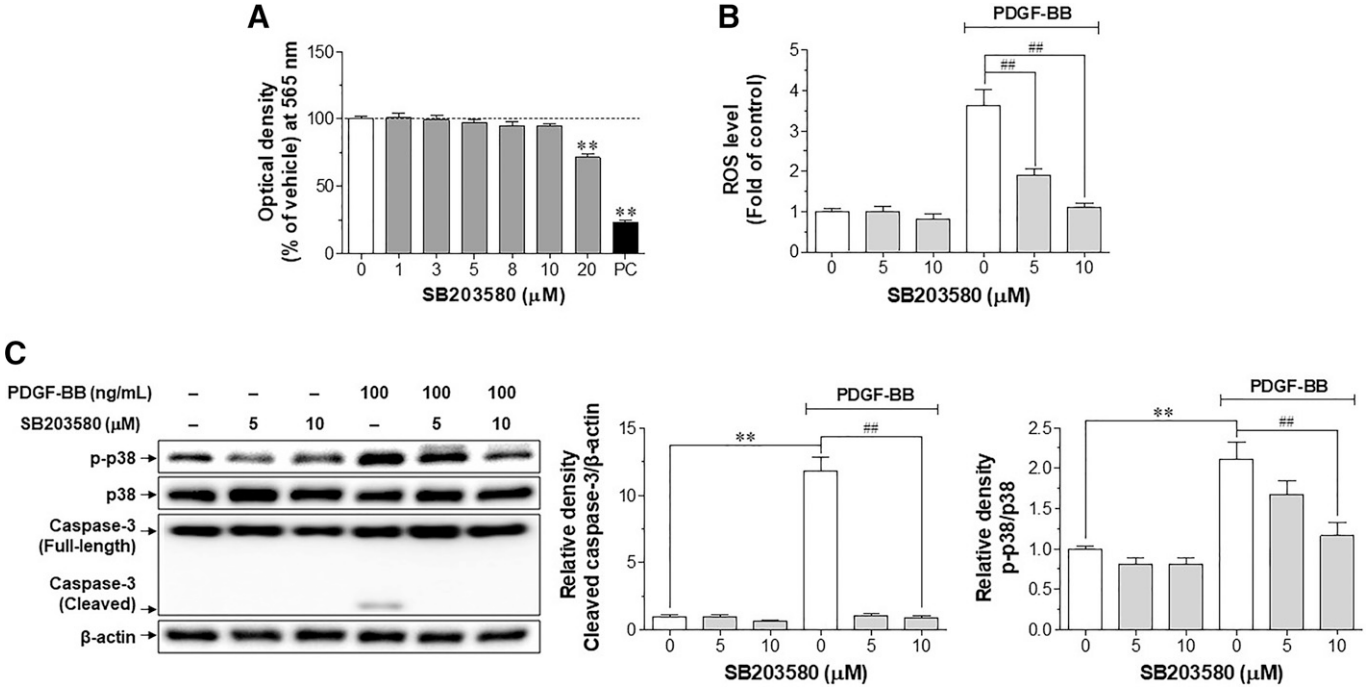

Fig. 6. Suppression of intracellular ROS levels and apoptosis by p38 inhibition. SB203580, a p38 inhibitor, was used to treat VSMCs. (A) The concentration of SB203580 used for the experiment was determined through MTT assay. Digitonin (100 μg/ml) was used as a positive control (PC). (B) The H_2DCFDA assay was used to measure intracellular ROS levels. VSMCs were pretreated with SB203580 (5 or 10 μM), after which PDGF-BB (100 ng/ml) was added for an additional 72 hours. (C) Cleaved caspase-3 levels and the phosphorylation of p38 (p-p38) were measured via Western blot analysis. The gel images are representative of three similar independent experiments. Data are expressed as the mean ± S.E.M. $^{**}P < 0.01$ vs. no treated control, $^{\#\#}P < 0.01$ vs. PDGF-BB (100 ng/ml)–treated control. $n = 3$ per group.

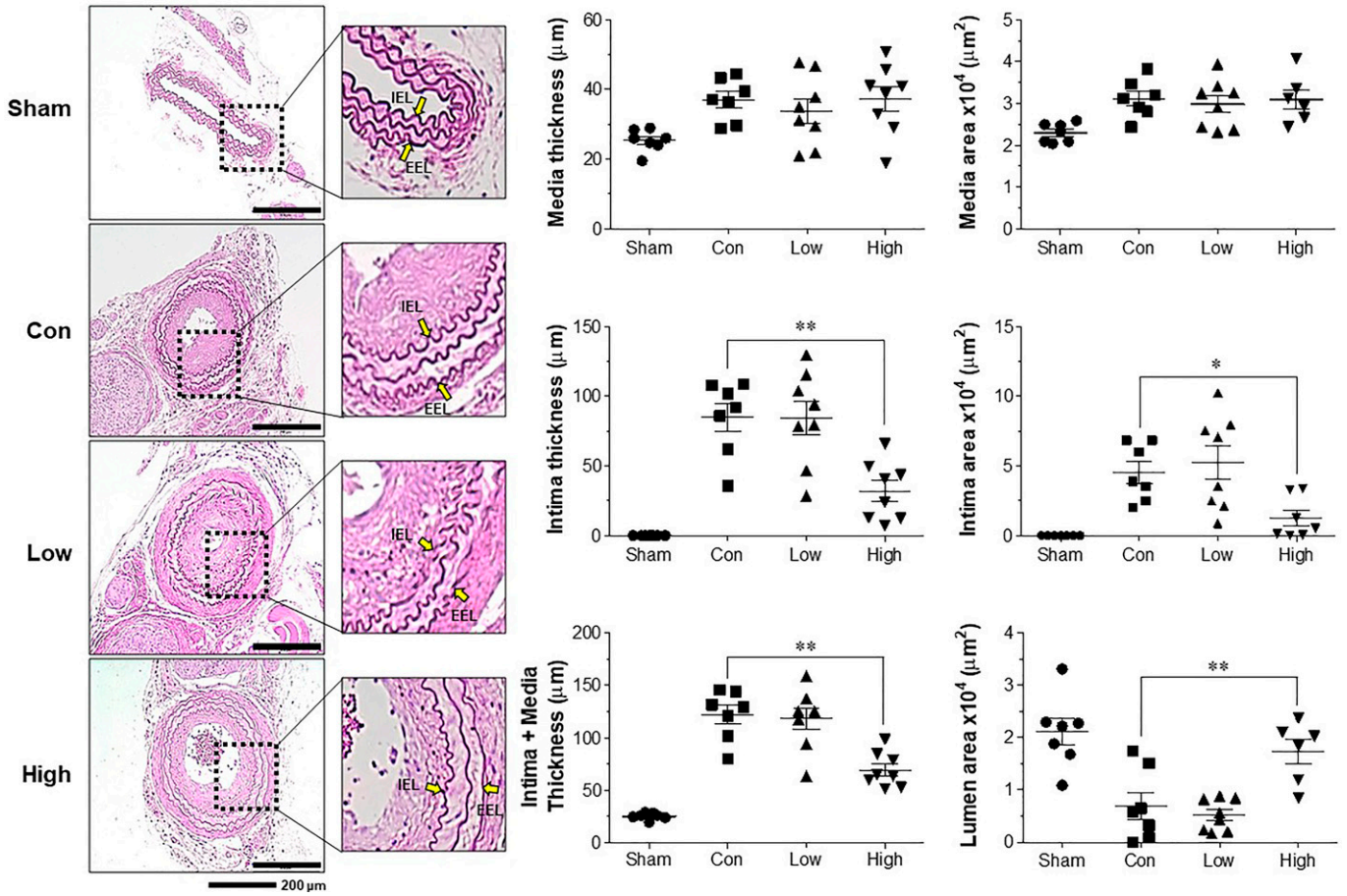

Fig. 7. Effect of rosuvastatin on the intima and media in a mouse model of carotid ligation. Low- or high-concentration rosuvastatin was orally administered beginning 2 days before ligation until 5 weeks after ligation. The body weights of the mice were not changed over the experimental period (data not shown). At 5 weeks after ligation, the carotid artery was harvested and fixed in paraffin, and H&E staining was performed. The thickness and area of the intima, media, and lumen were measured. The images shown are representative of those obtained from eight independent experiments. Data are expressed as the mean ± S.E.M (n = 8 for each experimental group). *$P < 0.05$; **$P < 0.01$ vs. control (Con). Sham refers to unligated, Con refers to ligated without rosuvastatin treatment, and Low refers to ligated and 1 mg/kg per day rosuvastatin. EEL, external elastic lamina; IEL, internal elastic lamina.

(10 mg/kg) reduced intima-media thickness and increased the area of the lumen in a ligated carotid artery mouse model.

Discussion

Atherosclerosis and its complications are some of the leading causes of death worldwide. For many years, atherosclerosis has been classified primarily as a lipid-induced disease characterized by lipid deposits on blood vessels, and research continues to focus on its prevention; however, the risk of complications remains high, and millions of people worldwide suffer from these complications each year (Schaftenaar et al., 2016). VSMCs are a cell type that constitutes blood vessels; however, their excessive proliferation, migration, and apoptosis induced by PDGF and inflammatory cytokines secreted from foam cells contribute to the development of atherosclerosis (Basatemur et al., 2019; Libby et al., 2019). Therefore, investigating the apoptosis of VSMCs in atherosclerosis is essential for developing treatment strategies.

The present study proposes a mechanism for the activity of rosuvastatin: rosuvastatin inhibits VSMC apoptosis caused by excessive and prolonged PDGF stimulation. Rosuvastatin was confirmed to inhibit the apoptosis of VSMCs induced by PDGF-BB. Our study showed the upregulation of LC3 and inhibition of p38 phosphorylation by autophagy activation. Through inhibiting p38 phosphorylation, intracellular ROS levels and apoptosis were reduced.

Statins are a class of drugs generally used to treat and prevent hyperlipidemia in cardiovascular patients. Because statins are mainly used in combination with other medications, their potential drug-drug interactions should be considered (Wiggins et al., 2016). This study examined rosuvastatin, which exhibits better potency than other statins (Lopez, 2005; Karlson et al., 2016). The effect of rosuvastatin on autophagy in cancer and neuroinflammation has been studied (Zeybek et al., 2011; McFarland et al., 2018). Previous research has shown that atorvastatin, one of the statin family, protects VSMCs from calcification induced by transforming growth factor-β1 stimulation by inducing autophagy through inhibition of the β-catenin pathway (Liu et al., 2014). However, information on the mechanism by which rosuvastatin affects PDGF-BB–stimulated VSMC apoptosis via autophagy was insufficient, necessitating the current study.

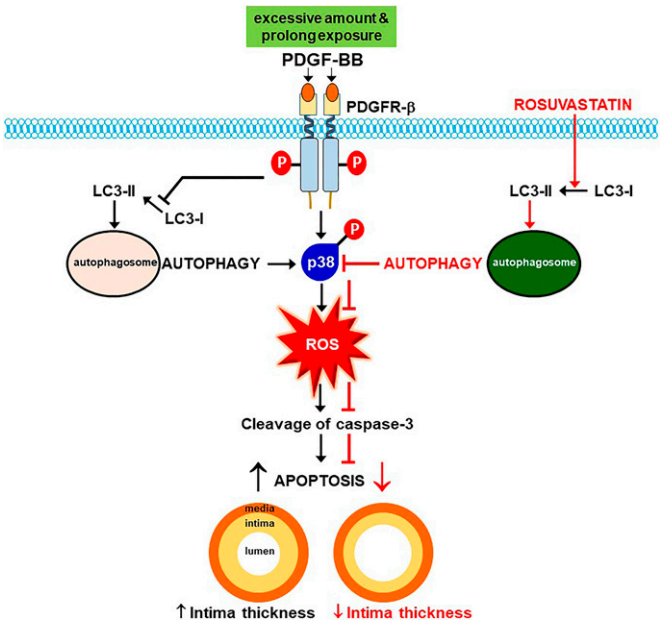

Fig. 8. Rosuvastatin reduces intracellular ROS level and apoptosis by inhibiting phosphorylation of p38 via autophagy in PDGF-BB–stimulated VSMCs. P, phosphoric acid.

PDGF-BB induces the proliferation and migration of VSMCs in the early stages of vascular disease (Ha et al., 2015), but cell apoptosis is induced when excessive stimulation with PDGF-BB is applied for long periods (Okura et al., 1998). Moreover, as a result of the absence of efficient phagocytosis, apoptotic VSMCs induce secondary necrosis (Bennett et al., 2012). Thus, cell death was assessed using Annexin V and 7-amino-actinomycin D (Muse Annexin V & Dead Cell Kit) as markers of dead VSMCs (Zembruski et al., 2012). PDGF-BB increased VSMC apoptosis and necrosis in a time- and concentration-dependent manner (Fig. 1, B and C). In addition, to evaluate apoptosis and secondary necrosis (caused by persistent apoptosis), the expression of cleaved caspase-3 and cleaved IL-1β was determined. The expression of cleaved caspase-3 (a major marker of apoptosis) was increased, and that of IL-1β (a major marker of secondary necrosis) was also increased by PDGF-BB stimulation (Fig. 1D). Simultaneously, rosuvastatin was found to concentration-dependently inhibit apoptosis and secondary necrosis induced by PDGF-BB (Fig. 1). The phosphorylation of p38, which is involved in the apoptosis pathway (Duan et al., 2016), was reduced by rosuvastatin (Fig. 3A). VSMCs induced apoptosis and thus secondary necrosis via prolonged stimulation with excessive PDGF-BB, whereas rosuvastatin reduced apoptosis by inhibiting the phosphorylation of p38.

Since the apoptosis of VSMCs induced by PDGF stimulation is accompanied by the generation of oxidative stress (Park et al., 2018), we evaluated the antioxidant activity of rosuvastatin by measuring its free radical scavenging ability and intracellular ROS levels. As a result of the DPPH assay, which was used to measure free radical scavenging (Sirivibulkovit et al., 2018), rosuvastatin was confirmed to lack significant free radical scavenging activity (Fig. 2A). Intracellular ROS levels, measured through the H_2DCFDA assay (Oparka et al., 2016), were initially increased by PDGF-BB stimulation and then decreased by rosuvastatin treatment (Fig. 2B). These results indicate that rosuvastatin has an antiapoptotic effect exerted by lowering the intracellular ROS level in VSMCs stimulated with PDGF.

In previous studies, autophagy was reported to regulate survival and function in VSMCs (Dong et al., 2019); thus, we examined the regulatory effect of rosuvastatin on autophagy. Rosuvastatin increased the expression of LC3 (Fig. 3C) and conversion of LC3-I to LC3-II (Fig. 3B). Furthermore, autophagy was confirmed to inhibit the apoptosis of VSMCs through the regulation of autophagy using 3-MA and rapamycin (Fig. 4). The phosphorylation of p38 was also inhibited by autophagy (Fig. 5). Thus, rosuvastatin inhibits p38 phosphorylation through autophagy, which can reduce apoptosis.

Using SB203580 (a specific inhibitor of p38 phosphorylation) (Yan et al., 2016), an experiment to determine whether the phosphorylation status of p38 affects intracellular ROS levels and apoptosis was conducted. Inhibition of p38 phosphorylation was confirmed to decrease the PDGF-induced increase in intracellular ROS level (Fig. 6B) and expression of cleaved caspase-3 (Fig. 6C). These results suggest that p38 phosphorylation status is related to the regulation of intracellular ROS and apoptosis induced by PDGF stimulation.

Intima and media thickness and area are now increasingly used experimentally as factors to assess the risk of atherosclerosis (Touboul et al., 2004; Park et al., 2017). In particular, intima-media thickness is known as a useful marker for predicting the occurrence of cardiovascular events (Touboul, 2015), and it is also used experimentally to evaluate carotid artery blood flow and luminal alteration in a carotid ligation animal model (Zhang et al., 2015). Therefore, we also used an established neointima formation model induced by carotid artery ligation to determine whether rosuvastatin would affect VSMCs proliferation in vivo (Brown et al., 2018). In a mouse model of carotid artery ligation, the media thickness and area were not altered by rosuvastatin, but the ligation-induced increases in intima thickness and area were diminished by rosuvastatin, thus increasing the area of the lumen, without toxicity (Fig. 7). In in vitro experiments, we used PDGF-BB with a high concentration of about 100 ng/ml, and the issue that this amount of PDGF-BB in cell levels is relevant to cause increased intimal thickness in vivo experiments is another part of research. In future studies, it may be necessary to compare plasma PDGF levels with control in the carotid ligation mouse model (or balloon-injury model) that causes neointima formations in experimental animals.

In conclusion, our study focused on the autophagy-mediated effect of rosuvastatin on VSMC apoptosis induced by PDGF stimulation. Our results indicated that rosuvastatin reduced intracellular ROS and apoptosis by inhibiting the phosphorylation of p38 via autophagy in PDGF-stimulated VSMCs (Fig. 8). In addition, it could suppress secondary necrosis caused by apoptosis accordingly. Therefore, the mechanism of rosuvastatin through autophagy could suggest a novel pathway for the treatment of vascular diseases such as atherosclerosis and restenosis in patients for whom conventional treatments have not been effective.

Authorship Contributions

Participated in research design: Jo, Park, Myung.
Conducted experiments: Jo, Park, Lee, Han, Myung.
Contributed new reagents or analytic tools: Heo.
Performed data analysis: Jo, Park, Myung.
Wrote or contributed to writing of the manuscript: Jo, Myung.

References

Altwairgi AK (2015) Statins are potential anticancerous agents (review). review *Oncol Rep* **33**:1019–1039.

Basatemur GL, Jørgensen HF, Clarke MCH, Bennett MR, and Mallat Z (2019) Vascular smooth muscle cells in atherosclerosis. *Nat Rev Cardiol* **16**:727–744.

Bennett M, Yu H, and Clarke M (2012) Signalling from dead cells drives inflammation and vessel remodelling. *Vascul Pharmacol* **56**:187–192.

Bennett MR, Sinha S, and Owens GK (2016) Vascular smooth muscle cells in atherosclerosis. *Circ Res* **118**:692–702.

Brown BA, Williams H, Bond AR, Angelini GD, Johnson JL, and George SJ (2018) Carotid artery ligation induced intimal thickening and proliferation is unaffected by ageing. *J Cell Commun Signal* **12**:529–537.

Cervantes Gracia K, Llanas-Cornejo D, and Husi H (2017) CVD and oxidative stress. *J Clin Med* **6**:22.

Dong Y, Chen H, Gao J, Liu Y, Li J, and Wang J (2019) Molecular machinery and interplay of apoptosis and autophagy in coronary heart disease. *J Mol Cell Cardiol* **136**:27–41.

Duan F, Yu Y, Guan R, Xu Z, Liang H, and Hong L (2016) Vitamin K2 induces mitochondria-related apoptosis in human bladder cancer cells via ROS and JNK/p38 MAPK signal pathways. *PLoS One* **11**:e0161886.

Ha JM, Yun SJ, Kim YW, Jin SY, Lee HS, Song SH, Shin HK, and Bae SS (2015) Platelet-derived growth factor regulates vascular smooth muscle phenotype via mammalian target of rapamycin complex 1. *Biochem Biophys Res Commun* **464**:57–62.

Heo KS, Fujiwara K, and Abe J (2014) Shear stress and atherosclerosis. *Mol Cells* **37**:435–440.

Kabeya Y, Mizushima N, Ueno T, Yamamoto A, Kirisako T, Noda T, Kominami E, Ohsumi Y, and Yoshimori T (2000) LC3, a mammalian homologue of yeast Apg8p, is localized in autophagosome membranes after processing. *EMBO J* **19**:5720–5728.

Karlson BW, Palmer MK, Nicholls SJ, Lundman P, and Barter PJ (2016) Doses of rosuvastatin, atorvastatin and simvastatin that induce equal reductions in LDL-C and non-HDL-C: Results from the VOYAGER meta-analysis. *Eur J Prev Cardiol* **23**:744–747.

Levine B and Kroemer G (2019) Biological functions of autophagy genes: a disease perspective. *Cell* **176**:11–42.

Libby P, Buring JE, Badimon L, Hansson GK, Deanfield J, Bittencourt MS, Tokgözoğlu L, and Lewis EF (2019) Atherosclerosis. *Nat Rev Dis Primers* **5**:56.

Lim S and Park S (2014) Role of vascular smooth muscle cell in the inflammation of atherosclerosis. *BMB Rep* **47**:1–7.

Liu D, Cui W, Liu B, Hu H, Liu J, Xie R, Yang X, Gu G, Zhang J, and Zheng H (2014) Atorvastatin protects vascular smooth muscle cells from TGF-β1-stimulated calcification by inducing autophagy via suppression of the β-catenin pathway. *Cell Physiol Biochem* **33**:129–141.

Liu Y, Sinha S, McDonald OG, Shang Y, Hoofnagle MH, and Owens GK (2005) Kruppel-like factor 4 abrogates myocardin-induced activation of smooth muscle gene expression. *J Biol Chem* **280**:9719–9727.

Lopez LM (2005) Rosuvastatin: a high-potency HMG-CoA reductase inhibitor. *J Am Pharm Assoc (2003)* **45**:503–513.

McFarland AJ, Davey AK, McDermott CM, Grant GD, Lewohl J, and Anoopkumar-Dukie S (2018) Differences in statin associated neuroprotection corresponds with either decreased production of IL-1β or TNF-α in an in vitro model of neuroinflammation-induced neurodegeneration. *Toxicol Appl Pharmacol* **344**:56–73.

Oishi Y and Manabe I (2016) Macrophages in age-related chronic inflammatory diseases. *NPJ Aging Mech Dis* **2**:16018.

Okura T, Igase M, Kitami Y, Fukuoka T, Maguchi M, Kohara K, and Hiwada K (1998) Platelet-derived growth factor induces apoptosis in vascular smooth muscle cells: roles of the Bcl-2 family. *Biochim Biophys Acta* **1403**:245–253.

Oparka M, Walczak J, Malinska D, van Oppen LMPE, Szczepanowska J, Koopman WJH, and Wieckowski MR (2016) Quantifying ROS levels using CM-H_2DCFDA and HyPer. *Methods* **109**:3–11.

Park HS, Han JH, Jung SH, Lee DH, Heo KS, and Myung CS (2018) Antiapoptotic effects of autophagy via ROS regulation in microtubule-targeted and PDGF-stimulated vascular smooth muscle cells. *Korean J Physiol Pharmacol* **22**:349–360.

Park HS, Quan KT, Han JH, Jung SH, Lee DH, Jo E, Lim TW, Heo KS, Na M, and Myung CS (2017) Rubiarbonone C inhibits platelet-derived growth factor-induced proliferation and migration of vascular smooth muscle cells through the focal adhesion kinase, MAPK and STAT3 Tyr^{705} signalling pathways. *Br J Pharmacol* **174**:4140–4154.

Pugsley HR (2017) Quantifying autophagy: measuring LC3 puncta and autolysosome formation in cells using multispectral imaging flow cytometry. *Methods* **112**:147–156.

Rossi E, Casali B, Regolisti G, Davoli S, Perazzoli F, Negro A, Sani C, Tumiati B, and Nicoli D (1998) Increased plasma levels of platelet-derived growth factor (PDGF-BB + PDGF-AB) in patients with never-treated mild essential hypertension. *Am J Hypertens* **11**:1239–1243.

Schaftenaar F, Frodermann V, Kuiper J, and Lutgens E (2016) Atherosclerosis: the interplay between lipids and immune cells. *Curr Opin Lipidol* **27**:209–215.

Sirivibulkovit K, Nouanthavong S, and Sameenoi Y (2018) Paper-based DPPH assay for antioxidant activity analysis. *Anal Sci* **34**:795–800.

Soulaidopoulos S, Nikiphorou E, Dimitroulas T, and Kitas GD (2018) The role of statins in disease modification and cardiovascular risk in rheumatoid arthritis. *Front Med (Lausanne)* **5**:24.

Tanida I, Ueno T, and Kominami E (2008) LC3 and autophagy. *Methods Mol Biol* **445**:77–88.

Touboul PJ (2015) Intima-media thickness of carotid arteries. *Front Neurol Neurosci* **36**:31–39.

Touboul P-J, Hennerici MG, Meairs S, Adams H, Amarenco P, Desvarieux M, Ebrahim S, Fatar M, Hernandez Hernandez R, Kownator S, et al.; Advisory Board of the 3rd Watching the Risk Symposium 2004, 13th European Stroke Conference (2004) Mannheim intima-media thickness consensus. *Cerebrovasc Dis* **18**:346–349.

Wiggins BS, Saseen JJ, Page 2nd RL, Reed BN, Sneed K, Kostis JB, Lanfear D, Virani S, and Morris PB; American Heart Association Clinical Pharmacology Committee of the Council on Clinical Cardiology; Council on Hypertension; Council on Quality of Care and Outcomes Research; and Council on Functional Genomics and Translational Biology (2016) Recommendations for management of clinically significant drug-drug interactions with statins and select agents used in patients with cardiovascular disease: a scientific statement from the American Heart Association. *Circulation* **134**:e468–e495.

Yan W, Xiaoli L, Guoliang A, Zhonghui Z, Di L, Ximeng L, Piye N, Li C, and Lin T (2016) SB203580 inhibits epithelial-mesenchymal transition and pulmonary fibrosis in a rat silicosis model. *Toxicol Lett* **259**:28–34.

Yang X, Yu DD, Yan F, Jing YY, Han ZP, Sun K, Liang L, Hou J, and Wei LX (2015) The role of autophagy induced by tumor microenvironment in different cells and stages of cancer. *Cell Biosci* **5**:14.

Zhang X, Zhang T, Gao F, Li Q, Shen C, Li Y, Li W, and Zhang X (2015) Fasudil, a Rho-kinase inhibitor, prevents intima-media thickening in a partially ligated carotid artery mouse model: Effects of fasudil in flow-induced vascular remodeling. *Mol Med Rep* **12**:7317–7325.

Zembruski NC, Stache V, Haefeli WE, and Weiss J (2012) 7-Aminoactinomycin D for apoptosis staining in flow cytometry. *Anal Biochem* **429**:79–81.

Zeybek ND, Gulcelik NE, Kaymaz FF, Sarisozen C, Vural I, Bodur E, Canpinar H, Usman A, and Asan E (2011) Rosuvastatin induces apoptosis in cultured human papillary thyroid cancer cells. *J Endocrinol* **210**:105–115.

Address correspondence to: Dr. Chang-Seon Myung, Department of Pharmacology, Chungnam National University College of Pharmacy, 99 Daehak-ro (St.), Yuseong-gu, Daejeon 34134, Republic of Korea. E-mail: cm8r@cnu.ac.kr